

Article

# End-to-End Delay Bound Analysis for VR and Industrial IoE Traffic Flows under Different Scheduling Policies in a 6G Network

Benedetta Picano <sup>\*,†</sup> and Romano Fantacci <sup>†</sup> 

Department of Information Engineering, University of Florence, Via di Santa Marta 3, 50139 Florence, Italy

\* Correspondence: benedetta.picano@unifi.it

† These authors contributed equally to this work.

**Abstract:** Next-generation networks are expected to handle a wide variety of internet of everything (IoE) services, notably including virtual reality (VR) for smart industrial-oriented applications. VR for industrial environments subtends strict quality of service constraints, requiring sixth-generation terahertz communications to be satisfied. In such an environment, an additional important issue is trying to get high utilization of network and computing resources. This implies identifying efficient access techniques and methodologies to increase bandwidth utilization and enable flows related to services, with different service requirements, to coexist on the same computation node. Towards this goal, this paper addresses the problem of coexistence of the traffic flows related to different services with given delay requirements, on the same computation node arranged to execute flow processing. In such a context, a theoretical comprehensive performance analysis, to the best of the authors' knowledge, is still missing in the literature. As a consequence, this lack strongly limits the possibility of fully capturing the performance advantages of computation node sharing among different traffic flows, i.e., services. The proposed analysis aims to give a measure of the ability of the system in accomplishing services before the expiration of corresponding deadlines. The integration of martingale bounds within the stochastic network calculus tool is provided, assuming both the first-in-first-out and the earliest deadline first scheduling policies. Finally, the validity of the analysis proposed is confirmed by the tightness emerging from the comparison between analytical predictions and simulation results.

**Keywords:** heterogeneous services; terahertz communications; stochastic network calculus



**Citation:** Picano, B.; Fantacci, R. End-to-End Delay Bound Analysis for VR and Industrial IoE Traffic Flows under Different Scheduling Policies in a 6G Network. *Computers* **2023**, *12*, 62. <https://doi.org/10.3390/computers12030062>

Academic Editor: Paolo Bellavista

Received: 25 January 2023

Revised: 6 March 2023

Accepted: 9 March 2023

Published: 13 March 2023



**Copyright:** © 2023 by the authors. Licensee MDPI, Basel, Switzerland. This article is an open access article distributed under the terms and conditions of the Creative Commons Attribution (CC BY) license (<https://creativecommons.org/licenses/by/4.0/>).

## 1. Introduction

Nowadays, in order to complete the intelligent industrial transition process, the Industrial Internet of Everything (IIoE) paradigm should play a crucial role, promoting the interaction of a large variety of devices with the surrounding environment, to support advanced intelligent decision-making strategies and disruptive services. In such a context, a class of services attracting increasing interest is that of the virtual reality (VR) in an IoE framework [1–3], enabled by sixth-generation (6G) technology. Upcoming 6G networks permit fast communications favoring real-time interaction between real-world entities and digital replicas [4–6], to support fast network reconfiguration and optimization. Systems handling the VR services are usually delay-sensitive, needs accurate investigation to properly manage the coexistence of the novel VR traffic, with preexisting workflows having the heterogeneous quality of service (QoS) requirements. The need for VR-supported environments typically also implies the usage of VR equipment (VE), such as head-mounted displays, demanding stereoscopic visual experience, or image rendering [4,5].

Although today's VE technology cannot support local rendering, in terms of limited battery lifetime, making even light rendering sessions impractical [4,7], the pervasive edge computing (PEC) approach now represents a promising paradigm, capable of supporting

VR-specific services at the edge of a network, close to the end users [4,7–10]. A PEC-based infrastructure can support rendering tasks, host offloaded tasks, lower the energy consumption of VE and, consequently, preserve battery lifetime [7]. On the one hand, THz communications represent a concrete technology to effectively satisfy strict service requirements regarding data rate constraints. Despite this, in a PEC structure shared by different services, fulfilling the strict requirements of the VR services, in terms of end-to-end (e2e) delay, is still a critical issue that needs to be carefully investigated.

In this regard, stochastic network calculus (SNC), based on min-plus algebra, represents an advanced tool to model and analyze computer network systems with complex traffic types, i.e., with general (GEN) distributions [11,12], and is suitable for the VR case.

The primary objective of this paper is to analytically derive the stochastic bound of the complementary cumulative distribution of the e2e delay, per flow, within a tandem system, based on a 6G network arranged to provide computation to new generation applications with heterogeneous QoS constraints. The bound formulated permits obtaining a measure of the system reliability, i.e., the ability of the system to provide e2e delay lower than a target threshold [13]. The main contributions of this paper can be summarized as follows:

- Performance measurement of a 6G-based computer network system, where the edge computing node is shared between two concurrent traffic flows, related to two different services, and, hence, having different e2e delay deadlines;
- Formulation of the per flow e2e delay bound for heterogeneous services (VR and industrial IoE), evaluating performance assuming different scheduling policies in order to identify the best solution. The formulation provided is pursued involving SNC theory applied with martingale envelopes describing traffic behavior.
- System performance validation, devoted to measuring the reliability of the network in completing services before corresponding flow deadlines and goodness of the obtained analytical predictions in comparison with simulations results.

Note that, whereas SNC is a powerful tool applied to a rich variety of problems and models, this paper contextualizes its application to new generation industrial networks that, to the best of the authors' knowledge, have not already been investigated in these terms. The rest of the paper is organized as follows. Section 2 details an in-depth review of the reference literature. Section 3 expresses the system model. Then, Section 4 describes the analysis formulated. In Section 5 the performance evaluation is presented, whereas conclusions are discussed in Section 6.

## 2. Related Works

Many works considered the problem of VR service provisioning, the objectives of which are described in Table 1. In particular, in [14] the authors focused on the network slicing problem, to guarantee ultra-reliable low latency communications and enhanced mobile broadband. Stochastic geometry was applied, in order to formulate the analysis. In [15], the combined problem of content caching and computational offloading was addressed, minimizing the mean transmission rate, considering the QoS requirements typical of VR application services. Authors in [16] jointly considered the problem of the satisfaction of both reliability and low latency, focusing on the design of massive multiple-input-multiple-output (MIMO) and multi-connectivity access protocol. Mission critical applications were the objective of the performance measurement provided in [17], in terms of packet error rate, proposing a framework considering the channel model and the transmission rate selection, and the learning model.

The implementation of a wireless sensors system was provided in [18], aiming at integrating the arranged network to operate VR services. A unified communication strategy was developed in paper [18] to lower the interference and the drawbacks stemming from heterogeneous sensing. Similarly, VR devices over wireless local area networks were deeply investigated in [19], focusing on the delay due to wireless channel fluctuations. A novel multi-user VR channel access scheme was proposed in [19] to minimize network delay.

Several papers focus on the evaluation of e2e delay exploiting the martingale theory. In particular, in [2,20] e2e analysis is presented by focusing only on the case of a single VR flow. The case of concurrent data flows related to different services accessing the same PEC structure is discussed in [21]. This paper considers a specific access scheme that requires a different formulation of the problem than the one of interest here, the main objective of which is to increase bandwidth utilization without losing the e2e delay constraints of the concurrent traffic. The derivation of an e2e delay bound is proposed in [22], where the multi-hop delay in vehicular ad hoc networks is studied, considering both access and queuing delays. In [23] the joint e2e delay of delay-tolerant and delay-sensitive bursty services is taken into account by applying the martingale analysis. The martingale bounds are also formulated in [24], where the analysis of ultra-reliable low latency and massive machine-type communications is presented. Authors in [24] based their analysis on the assumption of a multi-channel aloha type grant-free scheme, to maximize the throughput under some martingale bounds, which define the quality of service. The optimization problem applies the multi-variable-gray wolf optimizer algorithm. Finally, the martingale theory is also exploited in [13], where the authors propose the analysis of major random access schemes, in terms of both the packets backlog and delay.

**Table 1.** Related Literature.

Paper	Problem Addressed to Provide VR Services
[14]	Network slicing
[15]	Content caching and computational offloading
[16]	Design of a massive MIMO and a multi-connectivity access protocol
[17]	Packet error rate minimization
[18]	Implementation of a wireless sensors system
[19]	Network latency minimization
[22,23]	End-to-end delay minimization
[24]	Throughput maximization
[13]	Martingale-based random access protocols analysis

In this paper, an analytical framework, based on SNC principles and martingale envelopes, is proposed in order to analytically derive the e2e delay bound for VR applications in an industrial scenario where strict service requirements need to be addressed. Note that this is different from the focus of [16,17], which only looked at system reliability, and did not evaluate the impact of the e2e delay on performance achieved. Furthermore, the paper investigates the access delay impact on the resulting e2e performance in relation to the presence of concurrent heterogeneous traffic and different scheduling policies.

### 3. System Model

The reference scenario encompasses a Multi-access Edge Computing (MEC) system supporting the computation of traffic flows, heterogeneous in delay requirements, as shown in Figure 1. It is originated by one VR user with strict e2e delay requirements and a set  $\mathcal{B}$  of IoE devices. In particular, IoE devices are assumed here to be cyber-physical systems, i.e., systems that integrate sensing, computation, control, and networking into physical objects and infrastructure, having interacting capabilities with the MEC to offload tasks computation in order to make proper decisions regarding the monitoring and control of a process or physical environment. Data packet size is assumed to be the same for both flows, and the edge computing node, i.e., the MEC, located in the proximity of a Small Base Station (SBS) operating over 6G THz frequencies. Note that we refer to an intelligent industrial IoE environment, in which the IoE devices compose and monitor production plants, sensors, or industrial machinery, whose data support the VR user's experience through the exploitation of emerging simulating paradigms, for example, the digital twin [25]. VR users and IoE devices share a common access channel to the computation node, where the time is divided into slots of duration equal to the packets transmission time, assumed the same for the

two types of service. In particular, we focus here on the two power levels non-orthogonal multiple access (NOMA) cases where  $P_1$  and  $P_2$  are the two adopted power levels, with  $P_1 > P_2$  and  $P_1$  pre-assigned to the VR user, while  $P_2$  is assigned to the IIoE devices. A successive interference cancellation (SIC) receiver, as in [26,27], is used at the SBS site to detect data packets simultaneously transmitted on the same slot with different power levels. In particular, the SIC receiver implements an efficient multi-user detection procedure at the SBS site to reduce, or even eliminate, multi-access interference and, hence, allow successful reception of a target data packet. Accordingly, we considered the power levels  $P_1$  suitably defined in order to guarantee a safe detection when the VR user accesses the shared channel on a given slot and no more than one IIoE device accesses the channel (Note that this is a worst-case scenario for the VR flow, it usually being possible to guarantee correct detection even in the case of a number of IIoE devices accessing the shared channel on the same slot greater than 1). Likewise, the power level  $P_2$  was selected in order to guarantee correct detection of any IIoE data packet whenever no other IIoE devices access the shared channel on the same slot. (A deep discussion about the most suitable setting of the  $P_1$  and  $P_2$  power levels is, however, out of the scope of this paper. The interested reader can refer to [28] for more details on this issue). The analysis performed assumes a saturation condition, previously proposed in [29], for the IIoE traffic, which is a situation where the IIoE devices always have a new packet ready to be transmitted after any successful access attempt. In what follows, we also assumed that we had only one SBS, referred to as tagged SBS, which supports access (on the same THz channel) to VR and IIoE flows at the edge computing node in the proximity of the tagged SBS. Moreover, for the sake of simplicity, we assumed the VR user and IIoE devices were located at the same distance  $d_0$  from the tagged SBS; the differences between the effective distances being negligible for the purposes of our analysis.

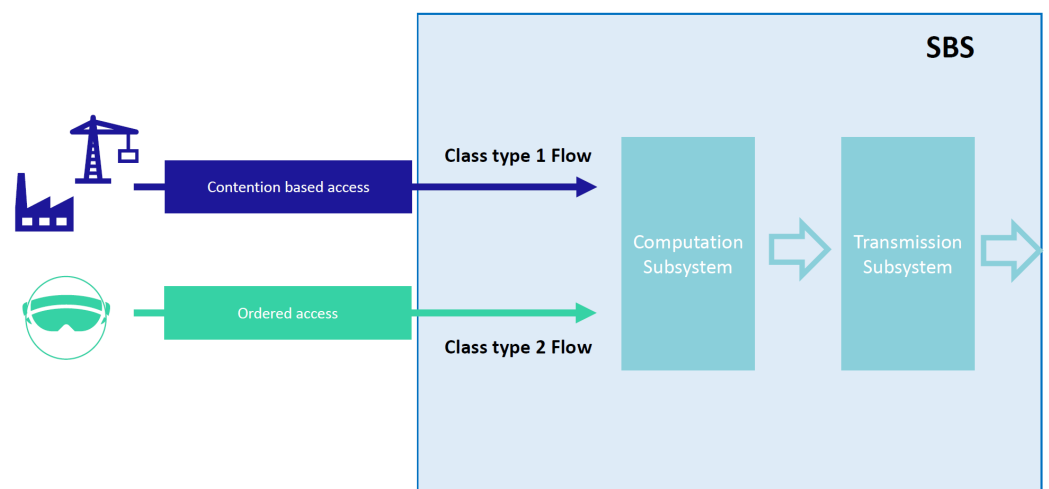


**Figure 1.** System Scenario: VR and IIoE services integrated at a Small Base Station (SBS).

### 3.1. Channel Model

In reference to [30], we considered a highly dense, short range communications environment, where the presence of an available line-of-sight (LoS) is always guaranteed for both the VR user and IIoE devices toward the SBS (Although our analysis was carried out under the assumption of guaranteed LoS conditions for both VR and IIoE devices, in Section 5 we relax this by considering the case in which NLoS propagation conditions occur with a certain probability). With the aim of adopting a unique data rate for both the VR and IIoE services uplink/downlink transmissions, we refer to the lowest allowable power level in the transmission, i.e.,  $P_2$ . Consequently, the common instantaneous rate,  $\mathcal{R}$ , for the

uplink/downlink error-free LoS communications between the tagged SBS and the linked VR user/IoE devices, results in [30,31]

$$\mathcal{R} = \mathcal{W} \log_2 \left( 1 + \frac{P_2 A_0 d_0^{-2} e^{-K(f)d_0}}{N_0} \right), \tag{1}$$

where  $\mathcal{W}$  is the bandwidth of the communication link and  $N_0$ , considering both the molecular absorption noise and the Johnson–Nyquist noise at the receiving site, results in

$$N_0 = \frac{\mathcal{W}\zeta}{4\pi} g_B T_0 + (P_1 + P_2) A_0 d_0^{-2} (1 - e^{-K(f)d_0}), \tag{2}$$

in which  $g_B$  is the Boltzmann constant,  $T_0$  is the temperature in Kelvin,  $\zeta$  the wavelength,  $K(f)$  the global absorption coefficient of the medium and  $A_0 = \frac{c^2}{16\pi^2 f^2}$  [30,31].

### 3.2. Channel Access Scheme

The VR user belonging to  $\mathcal{A}$ , having strict delay requirements typical of VR services, accesses the allocated channel, without contention, to the tagged SBS on a given slot, with probability  $p_t$ , and transmits data with the power level  $P_1$ . In contrast, the set  $\mathcal{B}$  contains  $v$  IIoE devices that can independently access the shared channel on each slot in contention mode. Each IIoE device can handle the transmission of only one packet at a time. In particular, a transmission success occurs when only one IIoE device transmits a data packet on a given slot. Conversely, a collision happens when two or more IIoE devices send out a data packet on the same slot, denying correct data packets reception at the MEC site. We adopted the Delayed First Transmission (DFT) approach, proposed and detailed in [29,32]. Hence, according to [29,32], the same transmission probability was considered for all packets to be sent by IIoE devices, regardless of the transmission attempt type (i.e., first or successive). This means that a new packet can be transmitted on a given slot with the same probability  $p_t$  as any other packet involved in collisions up to success. Finally, for the sake of analysis tractability, we assumed that the LoS link could not be lost once a transmission started.

### 4. End-To-End Delay Analysis

The e2e delay formulation is based on the system represented in Figures 2 and 3, depicting the tandem system taken into account here.

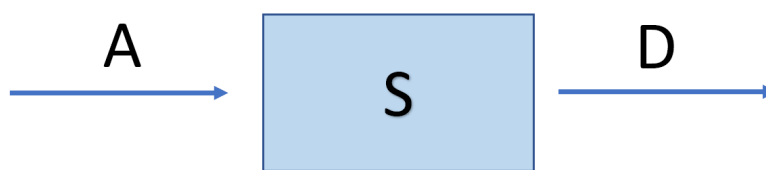


Figure 2. Single server scenario. A: arrival process, S: service process, D: departure process.

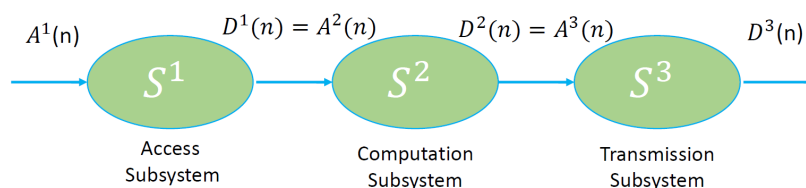


Figure 3. Tandem system model.

In what follows we refer to traffic of type 1 to denote the VR traffic, while traffic of type 2 represents the traffic injected into the network from the IIoE devices. Whenever

packet transmission occurs successfully, the packet goes through the MEC computation module, in accordance with the adopted queueing scheduling policy. After computation completion (i.e., service), each packet is sent back to the sender (VR user or IIoE device) through the transmission subsystem. The aggregate arrivals (i.e., VR and IIoE devices data packets)  $A$ , at the MEC, can be expressed by the following rule (3).

$$A = \begin{cases} 2, & p_s p_i \\ 1, & p_s(1 - p_i) + p_i(1 - p_s) \\ 0, & (1 - p_s)(1 - p_i). \end{cases} \quad (3)$$

where  $p_s = v p_i(1 - p_i)^{v-1}$  is the success probability for the IoE devices.

In compliance with the literature on this subject [13,33], service curves, describing the delay suffered by each flow in passing through the computation and the transmission subsystems, are formulated in the subsequent sections, for both the first-in-first-out (FIFO) and earliest deadline first (EDF) scheduling policies.

#### 4.1. Martingale Bound for FIFO Policy

Assuming a FIFO scheduling policy, requests are scheduled based on the arrivals of  $A^1$  and  $A^2$ , representing the arrivals of VR and IIoE device flows, respectively. Therefore, the service curves, for the two-class types flows are [34]

$$\begin{cases} S^{Type 1} = [S^{Tot}(m, n) - A^2(m, \hat{m})]_+ \mathbf{1}_{\hat{m} > x}, \\ S^{Type 2} = [S^{Tot}(m, n) - A^1(m, \hat{m})]_+ \mathbf{1}_{\hat{m} > x}, \end{cases} \quad (4)$$

where  $\hat{m} = n - x$ ,  $\hat{n} = n - m$ , whereas  $S^{Tot}$  denotes the service curve of the whole network. Through the min-plus convolution of the service curves of each server,  $x$  is a fixed parameter freely chosen, and  $\mathbf{1}$  is the indicator function, assuming value 1 if the condition  $n - m > x$  is satisfied, and zero otherwise. Without loss of generality, we can assume that flows and services admit martingale envelopes, denoting them as  $M_{A^1}$ ,  $M_{A^2}$ , and  $M_{S^i}$   $i \in \{2, 3\}$ , respectively, we can infer that [11,33,35]

$$D(n) \geq \inf_{0 \leq k \leq n} \{A^1(k) + S^2 \otimes S^3(l, n)\}, \quad (5)$$

and

$$D(n) \geq A^1 \otimes S^2 \otimes S^3(l, n). \quad (6)$$

Therefore,

$$\mathbb{P}(W(n) \geq k) \leq \mathbb{P}(\sup_{0 \leq k \leq n} \{A^1(k, n) - S^{Type 1}(n)\} \geq 0), \quad (7)$$

so we have

$$\mathbb{P}(W(n) \geq k) \leq \mathbb{P}(\sup_{0 \leq k \leq n} \{A^1(k, n) - [S^{Tot}(n) - A^2(n)]\} \geq 0). \quad (8)$$

Therefore,

$$\mathbb{P}(W(n) \geq k) \leq \mathbb{P}(\sup_{0 \leq k \leq n} \{A^1(k, n) + A^2(n) - S^{Tot}(n)\} \geq 0), \quad (9)$$

from which it follows that

$$\begin{aligned} \mathbb{P}(W(n) \geq k) &\leq \\ &\mathbb{P}(\sup_{0 \leq k \leq n} \{A^1(k, n) + A^2(n) - S^2(n) \otimes S^3(n)\} \geq 0). \end{aligned} \quad (10)$$

Assuming  $\tau_1 + \tau_2 = n$  and  $K^{S^2} = K^{S^3} = K_s$ , the envelopes are

$$M_{A^1} \approx h_{A^1}(a_n^1) e^{\theta(A^1(k,n) - (n-k)K^{A^1})}, \quad (11)$$

$$M_{A^2} \approx h_{A^2}(a_n^2) e^{\theta(A^2(k,n) - (n-k)K^{A^2})}, \quad (12)$$

$$M_{S^i} \approx h_{S^i}(s_{\tau_i}) e^{\theta(\tau_i K_s - S^i(\tau_i))}. \quad (13)$$

Due to the independence assumption, we can build the super-martingale process as the product of Equations (20)–(22) as

$$\mathcal{M} = \prod_{j \in \{A^1, A^2, S^2, S^3\}} M_j. \quad (14)$$

After some algebraic manipulations, and recalling that

$$\mathbb{E}[\mathcal{M}(k)] = \mathbb{E}[M_{A^1}(0) M_{A^2}(0) \prod_{j=2}^3 M_{S^j}], \quad (15)$$

it follows that

$$\mathbb{E}[\mathcal{M}(k)] \leq \mathbb{E}[M_{A^1}(0)] \mathbb{E}[M_{A^2}(0)] \prod_{j=2}^3 \mathbb{E}[M_{S^j}(0)]. \quad (16)$$

Consequently, the martingale bound is

$$\mathbb{P}(W(n) \geq k) \leq e^{-\theta^* k K_s} B, \quad (17)$$

in which

$$B = \frac{\mathbb{E}[M_{A^1}(0)] \mathbb{E}[M_{A^2}(0)] \mathbb{E}[M_{S^2}(0)] \mathbb{E}[M_{S^3}(0)]}{H}, \quad (18)$$

and  $H = \min\{h_{A^1}(a_n^1) h_{S^i}(s_{\tau_i}) : a_n - s_{\tau_i} > 0\}$ , and  $\theta^* = \sup\{\theta > 0 : K_a \leq K_s\}$ , as in [13].

#### 4.2. Martingale Bound for EDF Policy

The EDF policy considers the deadline associated with any (VR or IloE devices) traffic flow. In accordance with the EDF policy, the request processed is that having the smallest remaining deadline. In compliance with [36], the EDF scheduling for the two flow class types considered can be expressed as

$$\begin{cases} S^{Type 1} = [S^{Tot}(m, n) - A^2(m, \hat{m} + \min\{x, y\})] + \mathbf{1}_{\hat{m} > x}, \\ S^{Type 2} = [S^{Tot}(m, n) - A^1(m, \hat{m} + \min\{x, y\})] + \mathbf{1}_{\hat{m} > x}, \end{cases} \quad (19)$$

in which  $x$  is a fixed parameter freely chosen, and  $y$  is the difference between the two flow deadlines. The indicator function assumes value 1 if the condition  $n - m > x$  is satisfied, and zero otherwise.

As in the case of FIFO policy, the super-martingale process can be built, considering  $M_{A^1}$ ,  $M_{A^2}$  and  $M_{S^i}$  as

$$M_{A^1} \approx h_{A^1}(a_n^1) e^{\theta(A^1(k,n) - (n-k)K^{A^1})}, \quad (20)$$

$$M_{A^2} \approx h_{A^2}(a_n^2) e^{\theta(A^2(n-k+\min\{k,y\}) - (n-k+\min\{k,y\})K^{A^2})}, \quad (21)$$

$$M_{S^i} \approx h_{S^i}(s_{\tau_i}) e^{\theta(\tau_i K_s - S^i(\tau_i))} \quad (22)$$

In this case, we have to split the analysis based on two cases, corresponding to the situation in which  $y \geq 0$  and  $y < 0$ . When  $y \leq 0$ , we have  $\min\{k, y\} = y$ . Therefore, we can claim that

$$\mathbb{P}(W^1(n) \geq k) \leq \mathbb{P}\left(\sup_{0 \leq k \leq n} \{A^1(k, n) + A^2(n - k + y) - \sum_{i=2}^3 S^i(\tau_i)\} \geq 0\right). \quad (23)$$

A further distinction has to be made, considering the following cases

1.  $n \geq k, n < k - y$ ;
2.  $n \geq n - y$ ;

The case (1) implies the upper limitation of  $\mathbb{P}(W^1(n) \geq k)$  by (24),

$$\mathbb{P}\left(\sup_{k \leq n \leq n} \{A^1(k, n) + A^2(n - k)K^{A^1} + \sum_{i=2}^3 (\tau_i K_s - S^i(\tau_i))\} \geq kK_s\right), \quad (24)$$

from which we have

$$\mathbb{P}(W(n) \geq k) \leq e^{-\theta^* k K_s} B, \quad (25)$$

where

$$B = \frac{\mathbb{E}[M_{A^1}(0)]\mathbb{E}[M_{S^2}(0)]\mathbb{E}[M_{S^3}(0)]}{H}. \quad (26)$$

Analyzing the case (2), we have  $\mathbb{P}(W^1(n) \geq k)$  limited by (27).

$$\mathbb{P}\left(\sup_{k \leq n \leq n} \{A^1(k, n) + A^2(n - k + y) - (n - k)K^{A^1} - (n - k + y)K^{A^2} + \sum_{i=2}^3 (\tau_i K_s - S^i(\tau_i))\} \geq kK_s - yK^{A^1}\right). \quad (27)$$

By resorting to the super-martingale processes

$$\mathbb{P}(W^1(n) \geq k) \leq e^{-\theta^* k K_s - y K^{A^1}} B^*, \quad (28)$$

where

$$B^* = \frac{\mathbb{E}[M_{A^1}(0)]\mathbb{E}[M_{A^2}(0)]\mathbb{E}[M_{S^2}(0)]\mathbb{E}[M_{S^3}(0)]}{H}. \quad (29)$$

The final bound is expressed by

$$\mathbb{P}(W^1(n) \geq k) \leq e^{-\theta^* k K_s} B + e^{-\theta^* k K_s - y K^{A^1}} B^*. \quad (30)$$

Similarly, when  $y \geq 0$ , the bound results in

$$\mathbb{P}(W^2(n) \geq k) \leq e^{-\theta^* k K_s - \min\{k, y\} K^{A^1}} B^*, \quad (31)$$

where

$$B^* = \frac{\mathbb{E}[M_{A^1}(0)]\mathbb{E}[M_{A^2}(0)]\mathbb{E}[M_{S^2}(0)]\mathbb{E}[M_{S^3}(0)]}{H}, \quad (32)$$

Note that the analysis provided previously is devoted to measuring the delay suffered passing through the computation and transmission subsystems. Therefore, to derive the whole e2e delay bound, we have to consider different access delays for the two flow types. Due to the fact that we assumed the access contribution of the VR service request

deterministically equal to the computation request transmission time  $\tau$  (in *ms*), the target reliability deadline has to be scaled of  $\tau$  ms, hence

$$\mathcal{R} = 1 - \mathbb{P}(W(u) \geq \hat{k}), \quad (33)$$

in which  $\hat{k} = k - \tau$ . In reference to the IIoE devices, the e2e delay can be derived by (17) and (31), in which

$$B = \frac{\mathbb{E}[M_{A1}(0)]\mathbb{E}[M_{A2}(0)]\mathbb{E}[M_{S1}(0)]\mathbb{E}[M_{S2}(0)]\mathbb{E}[M_{S3}(0)]}{H}, \quad (34)$$

and

$$B^* = \frac{\mathbb{E}[M_{A1}(0)]\mathbb{E}[M_{A2}(0)]\mathbb{E}[M_{S1}(0)]\mathbb{E}[M_{S2}(0)]\mathbb{E}[M_{S3}(0)]}{H}, \quad (35)$$

assuming that  $S^1$  represents the service of the access subsystem as deeply discussed in [13], and summarized in Table 2.

**Table 2.** Bounds and advantages.

	<b>Bound</b>
EDF	$\mathbb{P}(W^1(n) \geq k) \leq \frac{e^{-\theta^* k K_s} B + e^{-\theta^* k K_s - y K^{A1}} B^*}{\mathbb{E}[M_{A1}(0)]\mathbb{E}[M_{A2}(0)]\mathbb{E}[M_{S2}(0)]\mathbb{E}[M_{S3}(0)]},$ with $B^* =$
FIFO	$\mathbb{P}(W(n) \geq k) \leq e^{-\theta^* k K_s} B$ with $B = \frac{\mathbb{E}[M_{A1}(0)]\mathbb{E}[M_{A2}(0)]\mathbb{E}[M_{S2}(0)]\mathbb{E}[M_{S3}(0)]}{H}$
Advantages	tightness between theoretical bound and simulation results

## 5. Performance Analysis

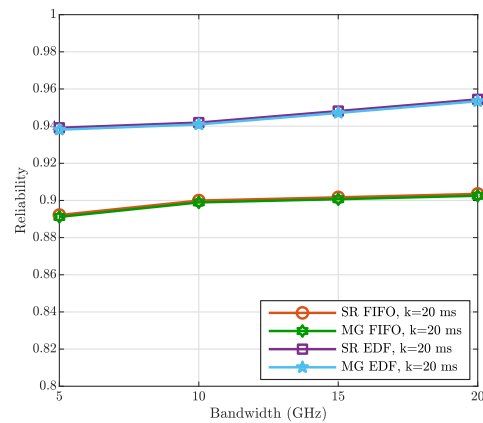
The experimental analysis exploited extensive numerical simulations, and the setting scenario (whose parameter values are reported in Table 3), was configured in compliance with realistic measures proposed in [37], where a squared network area, with a side of 20 m and service requests deadlines equal to 20 and 45 ms, was considered for the VR user and the IIoE devices traffic flow, respectively. The channel bandwidth, where not differently specified, was considered equal to 13 GHz. The computation time for the computing subsystem was assumed to be hyper-exponentially distributed with a mean computation time of 5.25 ms and having three components, as in [2]. Furthermore, the size of both VR and IIoE data packets were considered fixed and equal to 10 Mbits with the value of  $\tau$ , depending on the bandwidth of the allocated channels [37]. Finally, with the aim of making our simulations more closely related to real cases and compliant with the above working hypothesis, in performing our simulation it ran a NLoS probability, ( $P_{NLoS}$ ) equal to  $10^{-3}$ .

**Table 3.** Simulation Parameter Values.

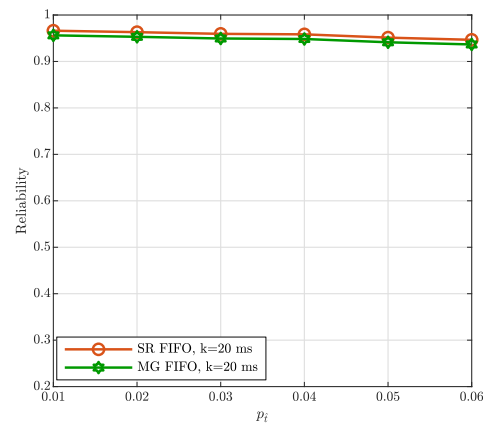
<b>Parameter</b>	<b>Values</b>
$f$	[0.2 THz, 1THz]
$K(f)$	$0.0016 \text{ m}^{-1}$
packet size	10 Mbits
$\beta$	20 ms
side of the network area	20 m
deadlines	20 and 25 ms
NLoS probability	$10^{-3}$
mean computation time	5.25 ms
$\mathcal{W}$	13 GHz
Water vapor percentage	1%

Figure 4 expresses the trend of the system performance, in terms of VR service reliability, as a function of the uplink/downlink channel bandwidth for both the FIFO and EDF policies. As is evident, the EDF policy provided remarkable benefits in comparison with the FIFO alternative. Furthermore, this figure highlights good agreement between the proposed martingale bounds (MGs) and the simulation results (SRs) for all the considered cases. From Figure 4, it is also evident that improvements on the transmission subsystem (i.e., increasing the bandwidth) did not drastically impact the overall system performance, especially in the case of FIFO policy. This is due to the fact that the computation subsystem represents the bottleneck of the tandem system. Figure 5 shows the VR service reliability behavior for  $p_t = 0$  as a function of  $p_{\hat{t}}$  and FIFO scheduling policy. We can note from the figure that the VR service reliability decreased as the VR traffic load, i.e.,  $p_{\hat{t}}$ , grew till the maximum value of 0.06, for a target service reliability value of 0.9; hence, resulting in a VR service throughput of 12 Gbits/s. Once again, the ability of analytical predictions in fitting actual SR results was evident. In particular, this validated the proposed analytical framework as an efficient tool to support an efficient design and parameter set for the considered system. Figure 6 depicts the VR service reliability as a function of the number of IoE devices linked to the same SBS, in the case of  $p_t = 0.025$  and  $p_{\hat{t}} = 0.01$ , considering a target VR service reliability not lower than 0.9. The figure highlights the advantages allowed by the EDF scheduling policy in comparison with the FIFO alternative. In particular, we noted an IoE service throughput of about 50% and an overall aggregated VR/IoE service throughput of 10,27 Gbits/s.

Similarly, Figure 7 illustrates the behavior of VR service reliability as a function of  $p_t$ . It is possible to note in this figure that performance degradation occurred as  $p_{\hat{t}}$  grew. The impact of the IIoE service deadline on the resulting service reliability is given in Figure 8, for  $p_t = 0.025$  and  $p_{\hat{t}} = 0.01$ . We note here that the IIoE service reliability increased when the associated deadline grew. Likewise, Figure 9 exhibits the outage probability for the IIoE devices, i.e., the probability that a IIoE task computation request is not accomplished within a given time deadline, as  $p_t$  grows. We would like to point out that the ability of the MG to accurately predict the actual behavior of the considered system is also evident in Figure 10, where the VR service reliability is expressed as a function of the available channel bandwidth. As a natural consequence, as the channel bandwidth increases, service requests transmission time drops and VR service reliability rises. Figure 11 depicts the VR service reliability for the case of 4 IIoE devices,  $p_t = 0.01$ , and variable  $p_{\hat{t}}$  values. This figure shows that it was possible to reach a VR service reliability greater than 0.9, even when  $p_{\hat{t}} = 0.01$ , producing a significant increment of the aggregated VR/IIoE service throughput. Finally, the impact of the terahertz propagation channel condition on the service reliability reached is provided in Figure 12, where the reliability curve is expressed as a function of the molecular absorption coefficient when  $p_t = 0$ ,  $p_{\hat{t}} = 0.001$ , and a FIFO policy is assumed. Note that we reported exclusively results for the FIFO policy case for the sake of the plot readability (i.e., values range reported on the y-axes). In conclusion, due to the tightness between the proposed MG bounds and the SR curves in both Figures 5–12, it is possible to state that the proposed analytical framework provides a powerful and useful tool to fully capture the performance advantages arising from efficient computation capability sharing among different services. In particular, we would like to stress that the good fitting between analytical predictions and simulation results was also achieved by considering a more realistic situation of a non-zero NLoS occurrence.



**Figure 4.** VR service reliability as a function of the channel bandwidth, considering  $p_t = 0.025$ , 3 IIoE devices and  $p_{\hat{t}} = 0.001$ .



**Figure 5.** VR service reliability as a function of  $p_{\hat{t}}$ , considering only the VR flow (i.e.,  $p_t = 0$ ).

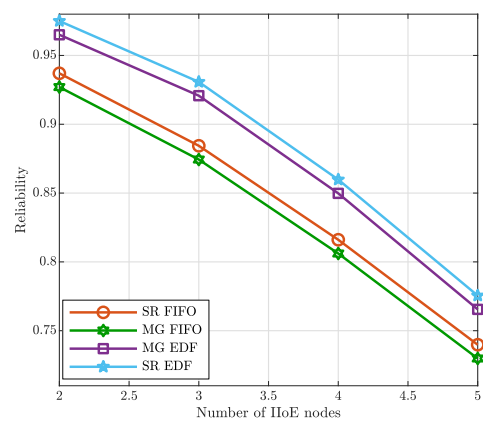


**Figure 6.** VR service reliability as a function of the number of IIoE devices, considering  $p_t = 0.025$  and  $p_{\hat{t}} = 0.01$ .

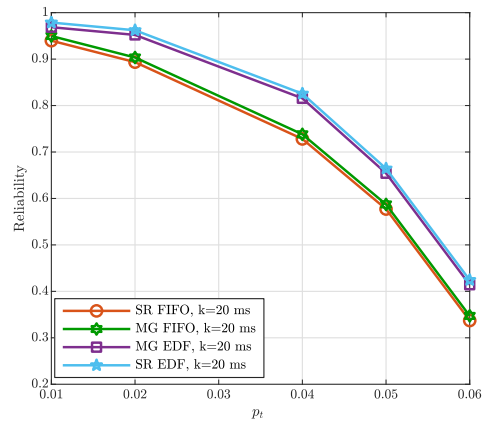


**Figure 7.** VR service reliability as a function of  $p_t$ , considering  $p_{\hat{t}} = 0.01$  and 3 IIoE devices.

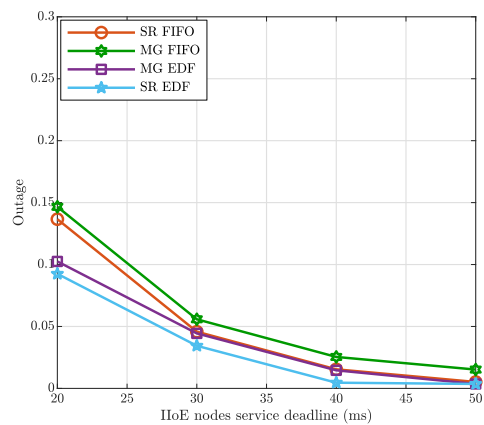


**Figure 8.** VR service reliability as a function of the deadline related to IIoE devices services, considering  $p_t = 0.025$  and  $p_{\hat{t}} = 0.01$ .

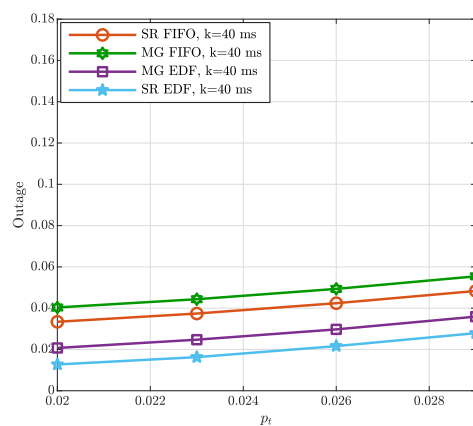


**Figure 9.** Outage as a function of  $p_t$ , considering  $p_{\hat{t}} = 0.01$ .

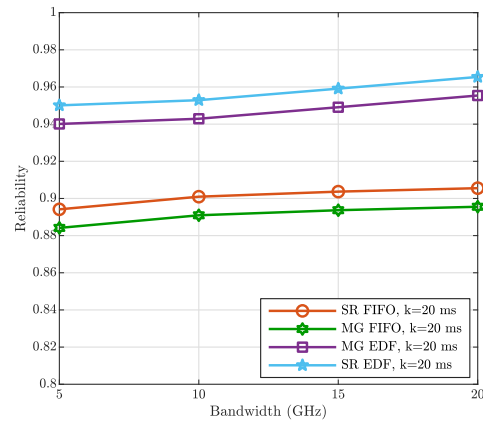


**Figure 10.** VR service reliability as a function of the bandwidth, considering  $p_t = 0.025$ , 3 IIoE devices and  $p_i = 0.001$ .

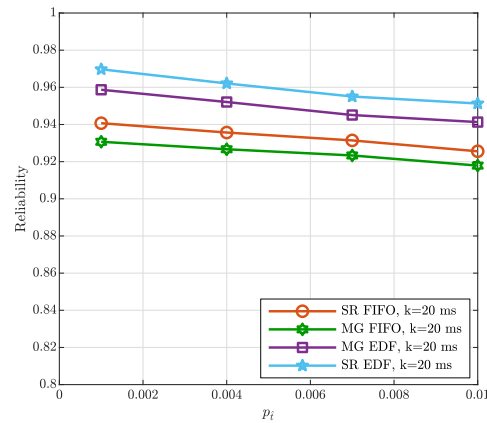


**Figure 11.** VR service reliability as a function of  $p_i$ , considering 4 IIoE devices and  $p_t = 0.01$ .

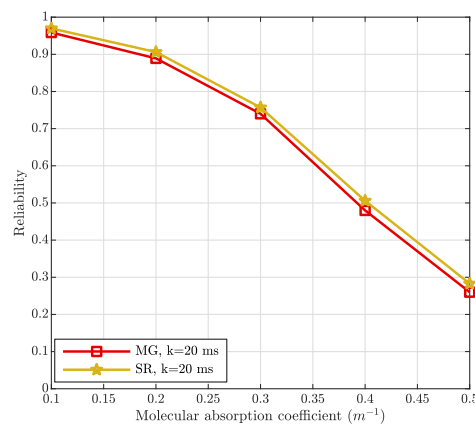


**Figure 12.** VR service reliability as a function of the molecular absorption, considering only the VR flow with  $p_i = 0.001$ .

Note that a significant limit of the proposed approach was that the difficulty of the analysis grew remarkably in the presence of more complex arrival processes, making the analysis infeasible.

## 6. Conclusions

This paper addressed the formulation of the e2e delay bound for VR/IoE services to support efficient computation capabilities sharing of an MEC node in the next generation, i.e., 6G, wireless networks in the THz bandwidth. The proposed e2e delay analysis proposes a combination of the SNC and the martingale theory, to model a stochastic bound of a tandem network representing the cascade system object of the analysis. Performance investigation had, as its main goal, assessment of the system reliability in guaranteeing the VR/IoE services, considering a THz network, under the assumption that VR and IoE services generate concurrent traffic to receive computation from the same MEC node. Two different scheduling policies were considered as alternatives, namely, the FIFO scheduling policy and the EDF scheduling policy. The results confirmed the validity of the proposed stochastic analysis in fitting the actual behavior and clearly demonstrated the advantages deriving from the adoption of the EDF solution, in comparison with the FIFO alternative, both in terms of achieved VR/IoE service reliability and aggregated overall system throughput. Future work may refer to the analysis of flows having different packet sizes, or tandem systems, where the backlog queue at the device site is included in the e2e delay analysis.

**Author Contributions:** Conceptualization, R.F.; writing—review & editing, R.F.; supervision, B.P. and R.F. All authors have contributed equally to the work. All authors have read and agreed to the published version of the manuscript.

**Funding:** This work was partially supported by the European Union under the Italian National Recovery and Resilience Plan (NRRP) of NextGenerationEU, partnership on “Telecommunications of the Future” (PE0000001—program “RESTART”).

**Institutional Review Board Statement:** Not applicable.

**Informed Consent Statement:** Not applicable.

**Conflicts of Interest:** The authors declare no conflict of interest.

## References

1. Wang, M.; Lin, Y.; Tian, Q.; Si, G. Transfer learning promotes 6g wireless communications: Recent advances and future challenges. *IEEE Trans. Reliab.* **2021**, *70*, 790–807. [[CrossRef](#)]
2. Fantacci, R.; Picano, B. End-to-end delay bound for wireless uvr services over 6g terahertz communications. *IEEE Internet Things J.* **2021**, *8*, 17090–17099. [[CrossRef](#)]
3. Picano, B.; Fantacci, R.; Han, Z. Nonlinear dynamic chaos theory framework for passenger demand forecasting in smart city. *IEEE Trans. Veh. Technol.* **2019**, *68*, 8533–8545. [[CrossRef](#)]
4. Gomes de Sa, A.; Zachmann, G. Virtual reality as a tool for verification of assembly and maintenance processes. *Comput. Graph.* **1999**, *23*, 389–403. [[CrossRef](#)]
5. Lin, P.; Song, Q.; Wang, D.; Yu, R.; Guo, L.; Leung, V. Resource management for pervasive edge computing-assisted wireless vr streaming in industrial internet of things. *IEEE Trans. Ind. Inform.* **2021**, *17*, 7607–7617. [[CrossRef](#)]
6. Qi, Y.-M.; Xie, B.; Deng, S.-P. Research on intelligent manufacturing flexible production line system based on digital twin. In Proceedings of the 2020 35th Youth Academic Annual Conference of Chinese Association of Automation (YAC), Zhanjiang, China, 16–18 October 2020; pp. 854–862.
7. Liu, Y.; Liu, J.; Argriou, A.; Ci, S. Mec-assisted panoramic vr video streaming over millimeter wave mobile networks. *IEEE Trans. Multimed.* **2019**, *21*, 1302–1316. [[CrossRef](#)]
8. Bastug, E.; Bennis, M.; Medard, M.; Debbah, M. Toward interconnected virtual reality: Opportunities, challenges, and enablers. *IEEE Commun. Mag.* **2017**, *55*, 110–117. [[CrossRef](#)]
9. Singh, P.; Singh, L.K. Reliability and safety engineering for safety critical systems: An interview study with industry practitioners. *IEEE Trans. Reliab.* **2021**, *70*, 643–653. [[CrossRef](#)]
10. Huang, C.-F.; Huang, D.-H.; Lin, Y.-K. Reliability evaluation of a cloud-fog computing network considering transmission mechanisms. *IEEE Trans. Reliab.* **2021**, *71*, 1355–1367. [[CrossRef](#)]
11. Fidler, M.; Rizk, A. A guide to the stochastic network calculus. *IEEE Commun. Surv. Tutor.* **2015**, *17*, 92–105. [[CrossRef](#)]
12. Jiang, Y. A basic stochastic network calculus. *SIGCOMM Comput. Commun. Rev.* **2006**, *36*, 123–134. [[CrossRef](#)]
13. Poloczek, F.; Ciucu, F. Service-martingales: Theory and applications to the delay analysis of random access protocols. In Proceedings of the 2015 IEEE Conference on Computer Communications (INFOCOM), Hong Kong, China, 26 April–1 May 2015; pp. 945–953.

14. Park, J.; Bennis, M. Ullc-emb slicing to support VR multimodal perceptions over wireless cellular systems. In Proceedings of the IEEE Global Communications Conference (GLOBECOM) 2018, Abu Dhabi, United Arab Emirates, 9–13 December 2018.
15. Sun, Y.; Chen, Z.; Tao, M.; Liu, H. Communication, computing and caching for mobile vr delivery: Modeling and trade-off. In Proceedings of the 2018 IEEE International Conference on Communications (ICC), Kansas City, MO, USA, 20–24 May 2018; pp. 1–6.
16. Popovski, P.; Stefanovic, C.; Nielsen, J.J.; de Carvalho, E.; Angjelichinoski, M.; Trillingsgaard, K.F.; Bana, A. Wireless access in ultra-reliable low-latency communication (urllc). *IEEE Trans. Commun.* **2019**, *67*, 5783–5801. [[CrossRef](#)]
17. Angjelichinoski, M.; Trillingsgaard, K.F.; Popovski, P. A statistical learning approach to ultra-reliable low latency communication. *IEEE Trans. Commun.* **2019**, *67*, 5153–5166. [[CrossRef](#)]
18. Faidley, G.; Hero, J.; Lee, K.; Lwakabamba, B.; Walstrom, R.; Chen, F.; Dickerson, J.; Rover, D.; Weber, R.; Cruz-Neira, C. Developing an integrated wireless system for fully immersive virtual reality environments. In Proceedings of the Eighth International Symposium on Wearable Computers, Arlington, VA, USA, 31 October–3 November 2004; Volume 1, pp. 178–179.
19. Ahn, J.; Kim, Y.Y.; Kim, R.Y. Delay oriented vr mode wlan for efficient wireless multi-user virtual reality device. In Proceedings of the 2017 IEEE International Conference on Consumer Electronics (ICCE), Las Vegas, NV, USA, 8–10 January 2017; pp. 122–123.
20. Fantacci, R.; Picano, B. Edge-Based Virtual Reality over 6G Terahertz Channels. *IEEE Netw.* **2021**, *35*, 28–33. [[CrossRef](#)]
21. Picano, B. End-to-End Delay Bound for VR Services in 6G Terahertz Networks with Heterogeneous Traffic and Different Scheduling Policies. *Mathematics* **2021**, *9*, 1638. [[CrossRef](#)]
22. Hu, Y.; Li, H.; Chang, Z.; Han, Z. End-to-end backlog and delay bound analysis for multi-hop vehicular ad hoc networks. *IEEE Trans. Wirel. Commun.* **2017**, *16*, 6808–6821. [[CrossRef](#)]
23. Hu, Y.; Li, H.; Han, Z. Delay bound analysis using martingale for multimedia dtn under heterogeneous network for high-speed trains. In Proceedings of the 2015 IEEE Global Communications Conference (GLOBECOM), San Diego, CA, USA, 6–10 December 2015; pp. 1–6.
24. Qi, R.; Chi, X.; Zhao, L.; Yang, W. Martingales-based aloha-type grant-free access algorithms for multi-channel networks with mmhc/urllc terminals co-existence. *IEEE Access* **2020**, *8*, 37608–37620. [[CrossRef](#)]
25. Ferko, E.; Bucaioni, A.; Behnam, M. Architecting digital twins. *IEEE Access* **2022**, *10*, 50335–50350. [[CrossRef](#)]
26. Ding, Z.; Lei, X.; Karagiannidis, G.K.; Schober, R.; Yuan, J.; Bhargava, V.K. A survey on non-orthogonal multiple access for 5g networks: Research challenges and future trends. *IEEE J. Sel. Areas Commun.* **2017**, *35*, 2181–2195. [[CrossRef](#)]
27. Seo, J.; Jung, B.C.; Jin, H. Nonorthogonal random access for 5g mobile communication systems. *IEEE Trans. Veh. Technol.* **2018**, *67*, 7867–7871. [[CrossRef](#)]
28. Yin, Y.; Peng, Y.; Liu, M.; Yang, J.; Gui, G. Dynamic user grouping-based noma over rayleigh fading channels. *IEEE Access* **2019**, *7*, 110964–110971. [[CrossRef](#)]
29. Mutairi, A.; Roy, S.; Hwang, G. Delay analysis of ofdma-aloah. *IEEE Trans. Wirel. Commun.* **2013**, *12*, 89–99. [[CrossRef](#)]
30. Jain, I.; Kumar, R.; Panwar, S. The impact of mobile blockers on millimeter wave cellular systems. *IEEE J. Sel. Areas Commun.* **2019**, *37*, 854–868. [[CrossRef](#)]
31. Petrov, V.; Moltchanov, D.; Koucheryavy, Y. Interference and sinr in dense terahertz networks. In Proceedings of the 2015 IEEE 82nd Vehicular Technology Conference (VTC2015-Fall), Boston, MA, USA, 6–9 September 2015; pp. 1–5.
32. Kleinrock, L.; Lam, S. Packet switching in a multiaccess broadcast channel: Performance evaluation. *IEEE Trans. Commun.* **1975**, *23*, 410–423. [[CrossRef](#)]
33. Liu, T.; Li, J.; Shut, F.; Han, Z. Quality-of-service driven resource allocation based on martingale theory. In Proceedings of the 2018 IEEE Global Communications Conference (GLOBECOM), Abu Dhabi, United Arab Emirates, 9–13 December 2018; pp. 1–6.
34. Fidler, M. An end-to-end probabilistic network calculus with moment generating functions. In Proceedings of the 2006 14th IEEE International Workshop on Quality of Service, New Haven, CT, USA, 19–21 June 2006; pp. 261–270.
35. Fidler, M. Survey of deterministic and stochastic service curve models in the network calculus. *IEEE Commun. Surv. Tutor.* **2010**, *12*, 59–86. [[CrossRef](#)]
36. Liebeherr, J.; Ghiassi-Farrokhfal, Y.; Burchard, A. On the impact of link scheduling on end-to-end delays in large networks. *IEEE J. Sel. Areas Commun.* **2011**, *29*, 1009–1020. [[CrossRef](#)]
37. Chaccour, C.; Soorki, M.; Saad, W.; Bennis, M.; Popovski, P. Can terahertz provide high-rate reliable low latency communications for wireless vr? *IEEE Internet Things J.* **2022**, *9*, 9712–9729. [[CrossRef](#)]

**Disclaimer/Publisher’s Note:** The statements, opinions and data contained in all publications are solely those of the individual author(s) and contributor(s) and not of MDPI and/or the editor(s). MDPI and/or the editor(s) disclaim responsibility for any injury to people or property resulting from any ideas, methods, instructions or products referred to in the content.